Expansion of human mesenchymal stem cells in a fixed-bed bioreactor system based on non-porous glass carrier – Part A: Inoculation, cultivation, and cell harvest procedures

Christian Weber, Denise Freimark, Ralf Pörtner, Pablo Pino-Grace, Sebastian Pohl, Christine Wallrapp, Peter Geigle, Peter Czermak

Published Version Information

Citation: Weber, C., Freimark, D., Pörtner, R., Pino-Grace, P., Pohl, S., Wallrapp, C., Geigle, P., Czermak, P. (2010). Expansion of human mesenchymal stem cells in a fixed-bed bioreactor system based on non-porous glass carrier – Part A: Inoculation, cultivation, and cell harvest procedures. International Journal of Artificial Organs, 33 (8), 512-525.

Digital Object Identifier (DOI):

Expansion of human mesenchymal stem cells in a fixed-bed bioreactor system based on non-porous glass carrier – Part A: Inoculation, cultivation, and cell harvest procedures

Short title: Expansion of hMSC in a fixed-bed bioreactor – Part A

Christian Weber

Institute of Biopharmaceutical Technology, University of Applied Sciences Giessen-Friedberg, Giessen, Germany

Denise Freimark

Institute of Biopharmaceutical Technology, University of Applied Sciences Giessen-Friedberg, Giessen, Germany

Ralf Pörtner

Institute of bioprocess and Biosystems Engineering, University of Technology, Hamburg, Germany

Pablo Pino-Grace

Institute of Biopharmaceutical Technology, University of Applied Sciences Giessen-Friedberg, Giessen, Germany

Sebastian Pohl

Institute of Biopharmaceutical Technology, University of Applied Sciences Giessen-Friedberg, Giessen, Germany

Christine Wallrapp

CellMed AG, Alzenau, Germany

Peter Geigle

CellMed AG, Alzenau, Germany

Peter Czermak

Institute of Biopharmaceutical Technology, University of Applied Sciences Giessen-Friedberg, Giessen, Germany

Department of Chemical Engineering, Kansas State University, Manhattan KS, USA

Corresponding author

Peter Czermak; Wiesenstraße 14, 35390 Giessen, Germany, phone +496413092634, fax +496413092553, e-mail peter.czermak@tg.fh-giessen.de

The Authors state that this manuscript has not been published previously and is not currently being assessed for publication by any journal other than the International Journal of Artificial Organs.

Each Author has contributed substantially to the research, preparation and production of the paper and approves of its submission to the Journal.

Abstract

Human mesenchymal stem cells (hMSC) are a promising cell source for several applications of regenerative medicine. The used cells are either autologous or allogenic, whereas the latter enables, especially by using of stem cell lines, a production of cell therapeutic or tissue engineered implants in stock. Therefore, the usually small initial cell number has to be increased. For that purpose bioreactors are demanded, which offer the controlled expansion of the hMSC under GMP-conform conditions.

In this study, divided in part A and B, a fixed bed bioreactor system based on non-porous borosilicate glass spheres for the expansion of hMSC, demonstrated with the model cell line hMSC-TERT, is introduced. The system offers a comfortable automation of the inoculation, cultivation, and harvesting procedures. Furthermore the bioreactor owns a simple design which benefits the manufacturing as disposable. Part A is focused on the inoculation, cultivation, and harvesting procedures. Cultivations were performed in lab scales up to a bed volume of 300 cm^3. It could be shown that the fixed bed system, based on 2-mm borosilicate glass spheres, as well as the inoculation, cultivation, and harvesting procedures are suitable for the expansion of hMSC with high yield and vitality.

Key words

mesenchymal stem cells, hMSC-TERT, fixed-bed reactor, glass carrier

Introduction

Due to their multipotency, mesenchymal stem cells can differentiate into various cell types like chondrocytes, neurocytes, myocytes, or osteocytes [1, 2] and are thus in focus of medicines and researchers. Autologous as well as allogenic cells can be used for regenerative medicine, whereas the allogenic cells have to be encapsulated to protect them from the host's immune system. However, the use of allogenic stem cells, especially stem cell lines, allows the production in shelf of cell therapeutic implants.

The expansion of mesenchymal stem cells from the initial cell number to an industrial relevant scale demands a bioreactor system that provides a gentle cultivation and harvest of the shear sensitive cells. Furthermore, the reactor system should be designed as a simple device that can be manufactured as disposable. The thereby saved cleaning and sterilization steps benefit the implementation of the system in GMP-conform processes. Additional important points concern the online monitoring of the cultivation status and the possibility of process automation.

A variety of bioreactor systems for the cultivation of diverse stem cell types have been described. It can be distinguished between static culture, often performed in cell culture plates or T-flasks [3-6], suspension reactors like spinner flasks [4, 7-9], stirred tanks or rotary bioreactors [6, 10-12], and perfusion reactors [4, 13-16]. Suspension and perfusion reactors require carrier or matrix systems which offer a suitable growth surface for the anchorage dependent cells. Cultivations of mesenchymal stem cells were performed, beside of T-flasks, in spinner flasks containing microcarrier (Cytodex® 1 and 3) [8], in rotary bioreactors [11], and in special reactors for stimulating the chondrogenic and osteogenic differentiation of encapsulated cells [4, 17]. The disadvantage by using static culture systems is the large labor input due to

the intricate automation of the inoculation, cultivation, and harvesting procedures. A better automation is feasible in suspension reactors, but the harvesting procedure and especially the separation process of the cells from the carrier is still intricate and means additional devices. This drawback can be overcome by using of fixed-bed reactors based on non-porous carrier. The non-porosity supports the separation of enzymatically detached cells from the immobilized carrier by flushing them out with the medium flow. Fixed-bed reactors can be simple designed, that benefits the production as disposable. Additionally an automation and process monitoring can easily be realized.

Up to now no cultivation of hMSC in fixed-bed reactors in order to expand the initial cell number has been described. In this work an axial fixed-bed reactor system for the cultivation of hMSC, which considers the requirements stated above, is introduced. The fixed-bed is based on non-porous borosilicate glass spheres with a diameter of 2 mm. These carriers are most suitable in respect to the nutrient supply and harvesting procedure as shown previously [18].

The used cells are human mesenchymal stem cells (hMSC), which are genetically modified with the gene of the catalytic subunit of human telomerase (TERT). This telomerase activity counteracts the shortening of the telomeres that occurs at each cleavage and thus leads to a permanent cell line [19].

Inoculation, cultivation, and harvesting procedures, which allow the automated generation of hMSC-TERT with high yield and vitality, were developed. Cultivations were performed in three different scales up to 300 cm^3 and cell densities of up to 2.9×10^6 cells/cm^3. The cultivation process was mathematically modeled in part B of this study. This enabled the theoretical scale up of the fixed-bed system which was exemplarily done for a target cell number of 20 billion. Cell dependent temporally

oxygen profiles were used for monitoring of the cultivation status. Growth and consumption kinetics were determined by fitting model parameters to the experimental data and in order to validate the model, from separate experiments in 6-well cell culture plates.

Materials and Methods

All chemicals were obtained from Sigma-Aldrich (Deisenhofen, Germany) unless otherwise indicated.

The hMSC-TERT cell line was provided by the CellMed Ag (Alzenau, germany). The passage numbers throughout the experiments were between 65 and 85.

All deviations resulted from repeated parallel experiments were expressed as standard deviation. Error propagations were considered using the Gaussian error propagation law. No further statistical evaluations were performed because of the small numbers of repeats of the cultivation runs.

The fixed-bed reactor system

The lab-scale fixed-bed reactors up to a bed volume V_{FB} of 60 cm^3 consisted of commercial glass syringes with special inserts, which replaced the original pistons (Figure 1 a, b) [20]. This perforated funnel shaped inserts, made of PEEK, offered a hose connector and thus enabled the perfusion of the packed beds with a homogenous inflow. A second custom-made system used for the 300 cm^3 scale was composed of a glass tube that was placed between stainless steel lid and bottom plates (Figure 1 c). These plates offered tube connections for the medium in- and outlet. A funnel shape insert for spreading of the incoming medium made up of stainless steel was placed in the inlet region. In both systems a stainless steel mesh avoided that the fixed bed enters the inlet tubing (Figure 1 a).

The fixed-bed reactors comprised non-porous borosilicate glass spheres with a diameter of 2 mm. This means a volume specific growth surface A_{FB} / V_{FB} of 18.3 cm^2/cm^3. A preliminary carrier screening with several porous and non-porous carriers

has revealed, that non-porous borosilicate glass spheres of 2 mm diameter are most suitable in respect to growth, cell harvest, and nutrient supply [18].

Three flasks equipped with sterile air filters for pressure compensation were connected to the fixed-bed reactor and acted as conditioning, inoculum, waste, and collecting vessel (Figure 1 d). The waste vessel contained the inoculum prior to the inoculation procedure. Oxygen concentration was measured in the medium in- and outflow using non-invasive oxygen sensors (Fibox 3, PreSens Precision Sensing GmbH, Augsburg, Germany). Medium was perfused by means of a peristaltic pump (IPC-8, Ismatec SA, Glattbrugg, Switzerland) and directed using pinch valves (100P NC 24-05, msscientific GmbH, Berlin, Germany). The reactor system was operated in a humidified incubator at 37°C and 5% CO_2. The medium was aerated in the conditioning vessel by surface aeration.

Static cell culture of hMSC-TERT

Cultivation in T-flasks

Stocks were thawed in a 37°C water bath until ice crystals completely disappeared. Afterwards cell suspensions were diluted in culture medium, which consisted of Eagles Minimal Essential Medium (EMEM; Biochrom, Berlin, Germany), supplemented with 10% fetal calf serum (FCS; Biowest, Nuaillé, France), at room temperature and centrifuged at 230 x g. After decantation of the supernatants, cells were resuspended in fresh medium, seeded into T300-flasks at a cell density of 5000 cells/cm^2, and cultured with 75 ml medium in a humidified incubator at 37°C and 5% CO_2 until a cell density of approximately 150,000 cells/cm^2 was reached. Medium was exchanged after three days of cultivation. Harvesting of cells was carried out by adding 0.05 ml/cm^2 trypsin-EDTA solution, incubation for 5 min, and rinsing of the

flasks with medium to stop the enzymatic reaction. Cells were used for experiments or subcultivated in T300-flasks after centrifugation and resuspension in medium.

Determination of growth and glucose consumption kinetics in 6-well cell culture plates

A Monod kinetic limitation by glucose was assumed. For determination of the dependency of the growth rate and glucose consumption rate on the glucose concentration four 6-well cell culture plates were inoculated with 5000 cell/cm^2 and cultured with 1 ml medium per well for eight days. Three wells were harvested daily and the cell numbers as well as the glucose concentrations were determined. The growth rate at each time interval

$$\Delta t^j = \left(t^j - t^{j-1}\right) \qquad \text{j = 1, 2, 3 … n}$$

was calculated by:

$$\mu^{\Delta t^j} = \frac{\ln\left(X_A^j\right) - \ln\left(X_A^{j-1}\right)}{t^j - t^{j-1}} \qquad \text{Equation 1}$$

This equation is only valid for the log phase of the cell growth, which was determined by taking the logarithm of the growth curve.

The glucose consumption was related to the logarithmic mean of the cell density $X_{A,m}^{\Delta t^j}$ in order to obtain the cell specific glucose consumption rate:

$$q_{Glc}^{\Delta t^j} = \frac{\left(c_{Glc}^{j-1} - c_{Glc}^{j}\right) \cdot V_{CV}}{\left(t^j - t^{j-1}\right) \cdot X_{A,m}^{\Delta t^j} \cdot A}$$ Equation 2

with the surface A, the glucose concentration c_{Glc}, and the medium volume V. The growth and consumption rates were plotted versus the logarithmic mean of the glucose concentration $c_{Glc,m}^{\Delta t^j}$ so as to obtain the Monod kinetics for the growth rate

$$\mu = \mu_{\max} \cdot \frac{c_{Glc}}{c_{Glc} + K_{M,\mu}}$$ Equation 3

and the glucose consumption rate

$$q_{Glc} = q_{Glc,\max} \cdot \frac{c_{Glc}}{c_{Glc} + K_{M,q_{Glc}}}$$ Equation 4

by curve fitting.

Dynamic cell culture of hMSC-TERT in the fixed bed systems

Inoculation procedure

The inoculation procedure was performed in different ways. In the first method a 14.2 cm^3 fixed bed was filled with cell suspension (10,000 cells per cm^2 growth surface area) and incubated for 90 min without perfusion. This method was then modified in order to return settled non-adhered cells into the fixed bed and thus increase the yield of adherent cells. For it the fixed bed was perfused for 7 min at a superficial velocity v of 1.2 x 10^{-4} m s^{-1} after time intervals of 30 min. This cycle was

repeated two or four times, so that the overall durations of these inoculation procedures were 104 and 178 min. The perfusion time was calculated from the fixed bed height h_{FB}, the superficial velocity v, and the factor 1.1, which means an overlap of the cell suspension over the fixed bed of 10%:

$$t_{perf} = 1.1 \cdot \frac{h_{FB}}{v} \qquad \text{Equation 5}$$

During the 30-min phases without perfusion the valve V1 (Figure 1 c) was closed to avoid a sedimentation of cells into the tubing. After the inoculation procedure, the fixed bed was rinsed with medium so as to get rid of non-adherent cells. The fixed beds were removed in layers to represent the axial cell density distribution. For determination of the cell number, nuclei were counted using a Neubauer hematocytometer after lysis of the cells with citric acid and staining with crystal violet as previously described [21]. The experiments were performed in triplicates.

Influence of the superficial velocity on the growth rate

Due to the non-porosity of the carrier, the cells are totally exposed to shear stress caused by the medium flow. This demands a determination of an upper limit for the superficial velocity v, which is important for an up-scaling of the process (see part B of this publication). The used criterion is the point at which the mean growth rate μ_m starts to decrease.

The investigations were carried out in four parallel-operated 14.2 cm^3 fixed-bed reactors. For that, fixed beds were inoculated as described above with 1.83 x 10^5

cells/cm^3 (10^4 cells/cm^2) and cultivated at three different superficial velocities v. For more details of these cultivations see Table 1. After cultivation, the fixed beds were removed in layers to represent the axial cell density distribution. Cell densities were determined by crystal violet staining of the nuclei at the end of the cultivations [21]. The mean growth rates were calculated according to Equation 1.

Cultivation in different fixed bed scales

Additional to the cultivation in 14.2 cm^3 fixed-bed reactors as described above, cultivations in a 60 cm^3 and 300 cm^3 scale were performed. The reactors were inoculated with 1.3 x 10^5 cells/cm^3 (7 x 10^3 cells/cm^2) and 1.8 x 10^5 cells/cm^3 (10 x 10^3 cells/cm^2), respectively, but it has to be noted, that this was not the initial cell density since only 50% of the inoculated cells got attached to the carrier as it will be shown subsequently. More details to the cultivations are given in Table 1. Cell densities were calculated from the oxygen consumption and determined by counting of the nuclei after cell lysis and crystal violet staining.

The cell numbers N_X^j at the time points t^j were calculated using the oxygen concentration difference between the in- and outlet $c_{Ox,in}^j - c_{Ox,out}^j$, the oxygen consumption rate q_{Ox} as well as the volume flow rate $\dot{V}$:

$$N_X^j = \frac{\left(c_{Ox,in}^j - c_{Ox,out}^j\right) \cdot \dot{V}}{q_{Ox}} \qquad \text{Equation 6}$$

For simplification, the oxygen uptake kinetic was considered as independent from the concentration and calculated with the oxygen difference between the medium in- and outlet at the end of the fixed bed cultivation:

$$q_{Ox} = \frac{\left(c^{n}_{Ox,CV} - s^{n}_{Ox,FB}\right) \cdot \dot{V}}{N^{n}_{X}} \qquad \text{Equation 7}$$

N^{n}_{X} is the cell number counted at the end of cultivation, $c^{n}_{Ox,CV}$ is the associated oxygen concentrations in the conditioning vessel and thus in the inlet of the fixed bed and $c^{n}_{Ox,FB}$ the outlet concentration.

From the cell densities X^{j}_{FB}, calculated with the cell number N^{j}_{X} and the fixed-bed volume V_{FB}, the initial cell density X^{0}_{FB} and the mean growth rate μ_m were obtained by curve fitting:

$$X_{FB} = X^{0}_{FB} \cdot e^{\mu_m \cdot t} \qquad \text{Equation 8}$$

The mean glucose consumption rate $q_{Glc,m}$ was calculated by the following equation

$$q_{Glc,m} = \frac{\left(c^{0}_{Glc} - c^{n}_{Glc}\right) \cdot V_{CV}}{X_{FB,m} \cdot V_{FB} \cdot t^{n}} \qquad \text{Equation 9}$$

with the medium volume in the conditioning vessel V_{CV}, the cultivation duration t^{n}, and the log mean of the cell density

$$X_{FB,m} = \frac{X_{FB}^{n} - X_{FB}^{0}}{\ln\left(\frac{X_{FB}^{n}}{X_{FB}^{0}}\right)}$$ Equation 10

Harvesting procedure

Investigations for the cell harvesting were performed in 14.2 cm^3 fixed-bed reactors at a cell density X_A of about 10^5 cells/cm^2. Accutase™ was mainly chosen because it is less harmful to the cells compared to trypsin. The investigated methods can be divided in two classes:

1. The enzyme solution and with it the detached cells were cyclic perfused with a comparably high superficial velocity v.
2. The enzyme solution was perfused at lower velocity and directly led to the collecting vessel. Then the detached cells were flushed out by means of perfusion of the fixed bed with medium at higher velocity, which was directed to the collecting vessel too.

The second procedure is assumed to be more gently because of the avoided recirculation of detached cells which causes less shear stress. More details to the harvesting experiments are given in Table 2. In order to avoid inhibiting effects of the serum to the enzyme activity the fixed beds were rinsed with 100 ml PBS in each case prior to enzymatic treatment.

Evaluation criteria for the harvesting procedures were the yield, which is defined as the number of detached cells to the overall cell number in the fixed bed, and the vitality, that is defined as the ratio of living cells to the total number of detached cells. Vitality was measured with the trypan blue exclusion method.

Results and Discussion

Growth and glucose uptake kinetics in 6-well cell culture plates

The glucose dependent growth and glucose consumption kinetics in static culture were obtained by fitting of Equation 3 and Equation 4 to the growth or consumption rate versus glucose concentration curves (Figure 2 and Figure 3). The maximal growth rate $\mu_{\max}$ and the Monod constant $K_{M,\mu_{Glc}}$ were found to be 0.66 ± 0.02 d^{-1} and 0.14 ± 0.03 mg ml^{-1}. The maximal glucose uptake rate $q_{Glc,\max}$ was (7.7 ± 1.1) x 10^{-8} mg h^{-1} $cell^{-1}$ with the according Monod constant $K_{M,q_{Glc}}$ = 0.16 ± 0.06 mg ml^{-1}.

It was assumed, that glucose is the limiting medium component. This assumption is corroborated by the fact, that the curve in Figure 3 passes the origin of the coordinates. A limitation by other nutrients like glutamine would shift the intersection with the x-coordinate. In addition, glutamine has been reported to be an unimportant energy source for human, goat, and rat mesenchymal stem cells [22].

The relation of lactate to consumed glucose is 2.74 mol/mol. This points at an inefficient metabolism of glucose for energy mainly via glycolysis. As well Schop et al. (2009) reported a high lactate/glucose ratio of up to 2.13 mol/mol at the cultivation of hMSC [22].

An oxygen limitation during the cultivation in cell culture plates can be excluded because of the high surface area to cell number relation. An estimation of the oxygen saturation of the medium at the highest cell density of 6.3 x 10^4 cells cm^{-2} using an oxygen transfer coefficient of 0.184 m h^{-1} [23] and an oxygen consumption rate of 2 x 10^{-8} mg h^{-1} $cell^{-1}$ leads to an saturation of about 99 %. Assuming a higher oxygen

consumption rate of 4 x 10^{-8} mg h^{-1} $cell^{-1}$ would only reduce the oxygen saturation to about 97 %.

Table 3 and Table 4 give some examples of published growth and glucose consumption kinetics of several animal and human cells or cell lines. The kinetics determined in this work are in the same range of those reported values.

Cultivation in fixed-bed reactors

Inoculation procedure

The yield of adherent cells after the inoculation procedure could have been increased by repeated perfusion of the fixed bed from 35 %, without perfusion, to 49% (Figure 4). No tendency dependent on the inoculation strategy regarding to the axial cell distribution could be detected.

Additional perfusion steps, another superficial velocities v, or time intervals between the perfusion steps could lead to a further enhancement of the yield of adherent cells. Thus, continuative studies are recommended.

Influence of the superficial velocity on the growth rate

The mean growth rate μ_m in the exponential phase decreases from 0.62 ± 0.01 d^{-1} at a superficial velocity v of 2.65 x 10^{-4} m s^{-1} to 0.29 ± 0.01 d^{-1} at a superficial velocity of 1.59 x 10^{-3} m s^{-1} (Figure 5). A flow velocity dependent trend in axial cell distribution could not be observed.

A mean growth rate μ_m of 0.62 d^{-1} is close to the maximal growth rate μ_{max} of 0.66 d^{-1}, determined in static culture in 6-well cell culture plates, which can only be reached by an infinite glucose concentration because of the Monod kinetic. Therefore it may be assumed, that a further decrease of superficial velocity v would not lead to

a significant increase in growth rate. For all of the subsequently performed cultivations, the rounded superficial velocity v of 3.0 x 10^{-4} m s^{-1} was used.

Cultivation of hMSC-TERT at different fixed bed scales

hMSC-TERT were cultured in scales V_{FB} of 14, 60, and 300 cm^3. Figure 6 to Figure 8 show the experimental data. The results are summarized in Table 5.

The cells were cultured up to a density X_{FB}^{n} of (2.93 ± 0.11) x 10^6 cells/cm^3. Higher cell densities are not recommendable because of the risk of channeling and drawbacks by up-scaling of the fixed bed system, as shown in part B of this publication. The initial cell densities X_{FB}^{0} and X_{A}^{0} were about 50 to 60% of the inoculated cell densities that confirms the results of the inoculation procedure.

The mean growth rate μ_{m} and the oxygen consumption rate q_{Ox} decreased with advancing passage number from 0.60 to 0.42 d^{-1} and 2,03 x 10^{-8} to 1,08 x 10^{-8} mg h^{-1} $cell^{-1}$, respectively, whereas the mean glucose consumption rate $q_{Glc,\mathrm{m}}$ increased from 7,65 x 10^{-8} to 9,50 x 10^{-8} mg h^{-1} $cell^{-1}$. Although hMSC-TERT are considered as a permanent cell line, changes in growth and consumption kinetics occur within 17 passages. A decrease of growth rate with advancing passage number has been reported for other cells like hMSC or adipose stem cells (rhesus monkey) [24, 25]. A consequence of this is that an optimized process design is only valid for a closed range of passage numbers.

All kinetics are within the range of those reported for several animal and human cells or cell lines (Table 3, Table 4, and Table 6).

For the oxygen uptake a zero order kinetic was assumed. This assumption is valid for an oxygen saturation above 20% and thus for the performed cultivation runs

[26]. Furthermore in part B of this study the constants of the growth kinetic μ_{max} and $K_{M,\mu_{Glc}}$ were determined by fitting model parameters to the experimental data of the fixed-bed cultivations [27]. Comparing the constants of the cultivation in the 14 cm^3 scale (passage number = 68) to those of the cultivation in 6-well cell culture plates (passage number = 69) of this publication no remarkable deviation in $K_{M,\mu_{Glc}}$ occurred. This suggests that the oxygen saturation has at least in the range of 35% to 100% a negligible effect on the growth kinetic. Otherwise the observable Monod constant $K_{M,\mu_{Glc}}$ for the glucose dependence of the growth rate would be wrongly increased.

Harvesting procedure

Increasing of the superficial velocity v of the cyclic perfused Accutase™ solution from 8.0 x 10^{-4} to 3.2 x 10^{-3} m s^{-1} and extension of the residence time from 10 to 20 min enhanced the yield from 5% to 76% (Figure 9, procedure a-c; Table 2). The vitality was 84%. Better results were obtained with non-cyclic perfusion of the enzyme solution and flushing out of the cells by a short time perfusion of the fixed bed with a comparably high superficial velocity (Figure 9, procedure d-i; Table 2). Treatment of the cells with Accutase™ solution for 10 min and a superficial velocity v of 1.8 x 10^{-4} m s^{-1} followed by perfusion with medium for 2 min and a superficial velocity of 3.2 x 10^{-3} m s^{-1} resulted in a yield of (82.1 ± 2.3)% and a vitality of (96.5 ± 0.7)%. Altogether, non-cyclic perfusion led to higher vitalities compared to cyclic perfusion, which is explainable by the reduced shear stress due to non-repeated passage of already detached cells through the system components.

Conclusion

The introduced fixed-bed reactor concept based on non-porous borosilicate glass spheres is suitable for the cultivation of hMSC-TERT. An application of the system for the cultivation of non-modified hMSC is supposable.

The introduced inoculation, cultivation, and harvesting procedures are designed for an automated performance of hMSC-TERT expansion with high yield and vitality of the harvested cells.

The simple designed reactor, which includes in principle a carrier filled tube connected to a conditioning vessel, enables a production of this system as disposable. An easy automation and a comfortable process monitoring by measuring of the oxygen concentration at the inlet and outlet or glucose concentration in the conditioning vessel, for example, benefit the transfer of this system into a GMP-process.

Acknowledgements

The authors would like to thank the Federal ministry of Economics and Technology for financial support as well as the CellMed AG for providing the production cell line hMSC-TERT.

References

[1] Barry, F.P. and J.M. Murphy. *Mesenchymal stem cells: clinical applications and biological characterization.* Int J Biochem Cell Biol. 2004; 36: 568-584

[2] Krampera, M., G. Pizzolo, G. Aprili and M. Franchini. *Mesenchymal stem cells for bone, cartilage, tendon and skeletal muscle repair.* Bone. 2006; 39: 678-683

[3] Oh, S.K.W., W.J. Fong, Y. Teo, H.L. Tan, J. Padmanabhan, A.C.P. Chin and A.B.H. Choo. *High density cultures of embryonic stem cells.* Biotechnol Bioeng. 2005; 91: 523-533

[4] Meinel, L., V. Karageorgiou, R. Fajardo, B. Snyder, V. Shinde-Patil, L. Zichner, D. Kaplan, R. Langer and G. Vunjak-Novacovic. *Bone tissue engineering using human mesenchymal stem cells: effects of scaffold material and medium flow.* Ann Biomed Eng. 2004; 32: 112-122

[5] Thomas, R.J., A. Chandra, Y. Liu, P.C. Hourd, P.P. Conway and D.J. Williams. *Manufacture of a human mesenchymal stem cell population using an automated cell culture platform.* Cytotechnology. 2007; 55: 31-39

[6] Lin, H.J., T.J. O'Shaughnessy, J. Kelly and W. Ma. *Neural stem cell differentiation in a cell– collagen– bioreactor culture system.* Dev Brain Res. 2004; 153: 163-173

[7] Abranches, E., E. Bekman, D. Henrique and J.M.S. Cabral. *Expansion of mouse embryonic stem cells on microcarriers.* Biotechnol Bioeng. 2006; 96: 1211-1221

[8] Frauenschuh, S., E. Reichmann, Y. Ibold, P.M. Goetz, M. Sittinger and J. Ringe. *A microcarrier-based cultivation system for expansion of primary mesenchymal stem cells.* Biotechnol Prog. 2007; 23: 187-193

[9] Sen, A., M.S. Kallos and L.A. Behie. *Effects of hydrodynamics on cultures of mammalian neural stem cell aggregates in suspension bioreactors.* Ind Eng Chem Res. 2001 40: 5350-5357

[10] Gerecht-Nir, S., S. Cohen and J. Itskovitz-Eldor. *Bioreactor cultivation enhances the efficiency of human embryoid body (hEB) formation and differentiation.* Biotechnol Bioeng. 2004; 86: 313-320

[11] Chen, X., H. Xu, C. Wan, M. McCaigue and G. Lia. *Bioreactor expansion of human adult bone marrow-derived mesenchymal stem cells (MSCs) .* Stem Cells. 2006; 24: 2052-2059

[12] Serra, M., C. Brito, S.B. Leite, E. Gorjup, H. von Briesen, M.J.T. Carrondo and P.M. Alves. *Stirred bioreactors for the expansion of adult pancreatic stem cells.* Ann Anatomy. 2009; 191: 104-115

[13] Bauwens, C., T. Yin, S. Dang, R. Peerani and P.W. Zandstra. *Development of a perfusion fed bioreactor for embryonic stem cell-derived cardiomyocyte generation: oxygen-mediated enhancement of cardiomyocyte output.* Biotechnol Bioeng. 2004; 90: 452-461

[14] Cho, C.H., J.F. Eliason and H.W.T. Matthew. *Application of porous glycosaminoglycan-based scaffolds for expansion of human cord blood stem cells in perfusion culture.* J Biomed Mat Res Part A. 2007; 86A: 98-107

[15] Jelinek, N., S. Schmidt, S. Thoma, C. Wandrey and M. Biselli, *Effects of collagenase on human hematopoietic cells* Animal cell technology: products from cells, cells as products - proceedings of the 16th ESACT meeting. 2000, Lugano, Switzerland: Bernard A., Griffiths B., Noé W., Wurm, F.

[16] Meissner, P., B. Schröder, C. Herfurth and M. Biselli. *Development of a fixed bed bioreactor for the expansion of human hematopoietic progenitor cells.* Cytotechnology. 1999; 30: 227-234

[17] Mauney, J.R., S. Sjosto, J. Blumberg, R. Horan, J.P. O - Novakovic, V. Volloch and V. Kaplan. *Mechanical stimulation promotes osteogenic differentiation of human bone marrow stromal cells on 3-D partially demineralized bone scaffolds in vitro.* Calcif Tissue Int. 2004; 74: 458-468

[18] Weber, C., S. Pohl, R. Poertner, P. Pino-Grace, D. Freimark, C. Wallrapp, P. Geigle and P. Czermak, *Production process for stem cell-based therapeutic implants - Expansion of the production cell line and cultivation of encapsulated cells*. Advances in Biochemical Engineering/Biotechnology, eds.: C. Kasper, M. van Griensven und R. Poertner, Vol. Bioreactor Systems for Tissue Engineering II - Strategies for stem cell expansion and differentiation. 2010, Berlin: Springer.

[19] Simonsen, J.L., C. Rosada, N. Serakinci, J. Justesen, K. Stenderup, S.I.S. Rattan, T.G. Jensen and M. Kassem. *Telomerase expression extends the*

proliferative life-span and maintains the osteogenic potential of human bone marrow stromal cells. Nat Biotechnol. 2002; 20: 592-596

[20] Weber, C., S. Pohl, R. Pörtner, C. Wallrapp, M. Kassem, P. Geigle and P. Czermak. *Cultivation and differentiation of encapsulated hMSC-TERT in a disposable small-scale syringe-like fixed bed reactor.* Open Biomed Eng J. 2007; 1: 64-70

[21] Weber, C., S. Pohl, R. Pörtner, C. Wallrapp, M. Kassem, P. Geigle and P. Czermak. *Expansion and harvesting of hMSC-TERT.* Open Biomed Eng J. 2007; 1: 38-46

[22] Schop, D., F.W. Janssen, L.D.S. van Rijn, H. Fernandes, R.M. Bloem, J.D. de Bruijn and R. van Dijkhuizen-Radersma. *Growth, metabolism, and growth inhibitors of mesenchymal stem cells.* Tissue Eng A. 2009; 15: 1877-1886

[23] Zimmermann, H.F. *Entwicklung der Hochdurchsatzfermentation: Bestimmung der bioverfahrenstechnischen Anforderungen und Implementierung der Laborautomation. Fakultät für Informatik und Elektrotechnik, University of Rostock;* PhD Thesis, 2005

[24] Lonergan, T., C. Brenner and B. Bavister. *Differentiation-related changes in mitochondrial properties as indicators of stem cell competence.* J Cell Physiol. 2006; 208: 149-153

[25] Weber, C., S. Gokorsch and P. Czermak. *Expansion and chondrogenic differentiation of human mesenchymal stem cells.* Int J Artif Organs. 2007; 30: 611-618

[26] Eibl, D., R. Eibl, R. Pörtner, G. Catapano and P. Czermak, *Cell and tissue reaction engineering*. 2009, Berlin-Heidelberg: Springer-Verlag.

[27] Weber, C., D. Freimark, R. Poertner, P. Pino-Grace, S. Pohl, C. Wallrapp, P. Geigle and P. Czermak. *Expansion of human mesenchymal stem cells in a fixed-bed bioreactors system - Part B: Modeling and scale up.* Int J Artif Organs 2010;

[28] Higuera, G., D. Schop, F. Janssen, R. van Dijkhuizen-Radersma, T. van Boxtel and C.A. van Blitterswijk. *Quantifying in vitro growth and metabolism kinetics of human mesenchymal stem cells using a mathematical model.* Tissue Eng Part A. 2009; 15: 1-11

[29] Conget, P. and J.J. Minguell. *Phenotypical and functional properties of human bone marrow mesenchymal progenitor cells.* J Cell Physiol. 1999; 181: 67-73

[30] Guo, Z., J. Yang, X. Liu, X. Li, C. Hou, P.H. Tang and N. Mao. *Biological features of mesenchymal stem cells from human bone marrow.* Chin Med J. 2001; 114: 950-953

[31] Liu, Y.-H., J.-X. Bi, A.-P. Zeng and J.-Q. Yuan. *A simple kinetic model for myeloma cell culture with consideration of lysine limitation.* Bioprocess Biosyst Eng. 2008; 31: 569-577

[32] Soukup, T., J. Mokrý, J. Karbanová, R. Pytlík, P. Suchomel and L. Kučerová. *Mesenchymal stem cells isolated from human bone marrow: cultivation, phenotypic analysis and changes in proliferation kinetics.* Acta Med. 2006; 49: 27-33

[33] Amit, M., M.K. Carpenter, M.S. Inokuma, C.P. Chiu and J.A. Thomson. *Clonally derived human embryonic stem cell lines maintain pluripotency and proliferative potential for prolonged periods of pulture.* Dev Biol. 2000; 227: 271– 278

[34] Breguet, V., R.I. Gugerli, U. von Stockar and I.W. Marison. *CHO immobilization in alginate/poly-L-lysine microcapsules: an understanding of potential and limitations.* Cytotechnology. 2007; 53: 81– 93

[35] Shirai, Y., K. Hashimoto and H. Takamatsu. *Growth kinetics of Hybridoma cells in high density culture.* J Ferment Bioeng. 1992; 73: 159-165

[36] Schop, D., F.W. Janssen, E. Borgart, J.D. de Bruijn and R. van Dijkhuizen-Radersma. *Expansion of mesenchymal stem cells using a microcarrier-based cultivation system: growth and metabolism.* J Tissue Eng Regen Med. 2008; 2: 126-135

[37] Boren, J., M. Cascante, S. Marin, B. Comın-Anduix, J.J. Centelles, S. Lim, S. Bassilian, S. Ahmed, W.N.P. Lee and L.G. Boros. *Gleevec (STI571) influences metabolic enzyme activities and glucose carbon flow toward nucleic acid and fatty acid synthesis in myeloid tumor cells.* J Biol Chem. 2001; 276: 37747– 37753

[38] Lubiniecki, A.S., *Large-scale mammalian cell culture technology*. Vol. 10. 1990: Marcel Dekker Inc.

[39] Peng, C.A. and B.A. Palson. *Determination of specific oxygen uptake rates in human hematopoietic cultures and implications for bioreactor design.* Ann Biomed Eng. 1996; 24: 373-381

[40] Acevedo, C.A., C. Weinstein-Oppenheimer, D.I. Brown, H. Huebner, R. Buchholz and M.E. Young. *A mathematical model for the design of fibrin microcapsules with skin cells.* Bioprocess Biosyst Eng. 2008; 32: 341-351

[41] De Leon, A., H. Mayani and O.T. Ramırez. *Design, characterization and application of a minibioreactor for the culture of human hematopoietic cells under controlled conditions.* Cytotechnology. 1998; 28: 127-138

[42] Youn, B.S., A. Sen and L.A. Behie. *Scale-up of breast cancer stem cell aggregate cultures to suspension bioreactors.* Biotechnol Prog. 2006; 22: 801-810

[43] Shirai, Y., K. Hashimoto, H. Yamaji and H. Kawahara. *Oxygen uptake rate of immobilized growing hybridoma cells.* Appl Microbiol Biotechnol. 1988; 29: 113-118

Nomenclature

A growth surface [m^2]

A_{FB} overall growth surface of the fixed bed [m^2]

c_{Glc} glucose concentration [kg m^{-3}]

c_{Glc}^{0} initial glucose concentration [kg m^{-3}]

c_{Glc}^{n} glucose concentration at the end of the cultivation (time point t^n) [kg m^3]

$c_{Glc,CV}$ glucose concentration in the conditioning vessel [kg m^{-3}]

$c_{Glc,m}^{\Delta t^j}$ logarithmic mean of the glucose concentration in the time interval Δt^j [kg m^{-3}]

$c_{Lac,CV}$ lactate concentration in the conditioning vessel [kg m^{-3}]

c_{Ox}^{*} maximal dissolved oxygen [kg m^{-3}]

$c_{Ox,CV}$ oxygen concentration in the conditioning vessel (fixed-bed inlet) [%]

$c_{Ox,FB}$ oxygen concentration in the fixed-bed outlet [%]

h_{FB} fixed bed height [m]

$K_{M,\mu}$ Monod constant for the growth kinetic [kg m^{-3}]

$K_{M,q_{Glc}}$ Monod constant for the glucose consumption kinetic [kg m^{-3}]

N_X cell number [-]

N_X^j cell number at the time point t^j [-]

N_X^n cell number at the end of cultivation (time point t^n) [-]

q_{Glc} glucose consumption rate [kg s^{-1} $cell^{-1}$]

$q_{Glc}^{\Delta t^j}$ glucose consumption rate in the time interval Δt^j [kg s^{-1} $cell^{-1}$]

$q_{Glc,\mathrm{m}}$ mean glucose consumption rate [kg s^{-1} $cell^{-1}$]

$q_{Glc,\max}$ maximal glucose consumption rate [kg s^{-1} $cell^{-1}$]

q_{Ox} oxygen consumption rate [kg s^{-1} $cell^{-1}$]

$s_{Ox,CV}$ oxygen saturation in the conditioning vessel (fixed-bed inlet) [%]

$s_{Ox,FB}$ oxygen saturation in the fixed-bed outlet [%]

t_{perf} time of perfusion [s]

v superficial velocity [m s^{-1}]

V volume [m^3]

$\dot{V}$ flow rate [m^3 s^{-1}]

V_{FB} fixed bed volume [m^3]

V_{CV} medium volume (conditioning vessel) [m^3]

X_A area related cell density [m^{-2}]

$X_{A,m}^{\Delta t^j}$ logarithmic mean of the area related cell density in the time interval Δt^j [m^{-2}]

X_{FB} volume related cell density [m^{-3}]

X_{FB}^{n} cell density at the end of cultivation [m^{-3}]

$X_{FB,m}^{\Delta t^j}$ logarithmic mean of the volume related cell density in the time interval Δt^j [m^{-3}]

Δt^j time interval $t^j - t^{j-1}$ j = 1, 2, 3 … n

μ growth rate [s^{-1}]

μ_m mean growth rate [s^{-1}]

μ_{max} maximal growth rate [s^{-1}]

$\mu^{\Delta t^j}$ growth rate in the time interval Δt^j [s^{-1}]

Legends

Figure 1: Fixed bed bioreactor systems for the expansion of hMSC-TERT.

a) Custom made insert for enabling the usage of commercial available syringes as fixed bed bioreactors

b) Syringe based small-scale fixed-bed reactor filled with 2 mm borosilicate glass spheres

c) Fixed bed bioreactor in a up to 500-cm^3 scale filled with 2-mm borosilicate glass spheres

d) Scheme of the bioreactor periphery

Figure 2: Monod kinetic of the growth rate (medium volume per well = 1.0 ml). The data represents the mean ± standard deviation (SD) of triplicates.

Figure 3: Monod kinetic of the glucose consumption rate (medium volume per well = 1.0 ml). The data represents the mean ± standard deviation (SD) of triplicates.

Figure 4: Yield of adherent cells and axial cell density distribution obtained by application of different inoculation procedures. Perfusion steps with a superficial velocity v of 1.2×10^{-4} m s^{-1} were applied for 7 min in time intervals of 30 min. The data represents the mean ± standard deviation of triplicates.

Figure 5: Axial cell density distributions and mean growth rates μ_m after six days of cultivation of hMSC-TERT in 14.2-cm^3 fixed-bed reactors at different superficial velocities v. The fixed beds consisted of 2 mm borosilicate glass spheres. The data represent the mean ± SD of three cultivations in each case.

Figure 6: Experimental data of a hMSC-TERT cultivation in four parallel operated fixed-bed reactors with a volume of each 14.2 cm^3. The reactors were connected to one conditioning vessel. Oxygen saturation was measured in the in and outlet of only one fixed-bed reactor. The data point of the counted cell number represents the mean ± SD of the four reactors. The reactors were perfused with a superficial velocity v of 2.7 x 10^{-4} m s^{-1}. The conditioning vessel contained 1000 ml EMEM + 10% FCS.

Figure 7: Experimental data of a hMSC-TERT cultivation in a 60-cm^3 fixed-bed reactor. The reactors were perfused with a superficial velocity v of 3.0 x 10^{-4} m s^{-1}. The conditioning vessel contained 500 ml EMEM + 10% FCS.

Figure 8: Experimental data of a hMSC-TERT cultivation in a fixed-bed reactor with a volume of 300 cm^3. The conditioning vessel contained 4800 ml EMEM + 10% FCS.

Figure 9: Yield and vitality of hMSC-TERT obtained with different harvesting procedures.

n: number of trials, t_e: duration of perfusion with the enzyme solution, t_m: duration of perfusion with the medium, v_e: superficial velocity during incubation with the enzyme solution, v_m: superficial velocity during the perfusion with medium

a) Accutase™; v_e = 8.0 x 10^{-4} m s^{-1}; t_e = 10 min; n = 1

b) Accutase™; v_e = 1.6 x 10^{-3} m s^{-1}; t_e = 10 min; n = 1

c) Accutase™; v_e = 3.2 x 10^{-3} m s^{-1}; t_e = 20 min; n = 1

d) Accutase™; v_e = 1.8 x 10^{-4} m s^{-1}; v_m = 1.6 x 10^{-3} m s^{-1}; t_e = 10 min; t_m = 1 min; n = 3

e) Accutase™; v_e = 1.8 x 10^{-4} m s^{-1}; v_m = 1.6 x 10^{-3} m s^{-1}; t_e = 10 min; t_m = 2 min; n = 2

f) Accutase™; v_e = 1.8 x 10^{-4} m s^{-1}; v_m = 3.2 x 10^{-3} m s^{-1}, t_e = 10 min; t_m = 1 min; n = 2

g) Accutase™; v_e = 1.8 x 10^{-4} m s^{-1}; v_m = 3.2 x 10^{-3} m s^{-1}; t_e = 10 min; t_m = 2 min; n = 2

h) Accutase™/trypsin; v_e = 1.8 x 10^{-4} m s^{-1}; v_m = 1.6 x 10^{-3} m s^{-1}; t_e = 10 min; t_m = 2 min; n = 2

i) Accutase™/trypsin; v_e = 1.8 x 10^{-4} m s^{-1}; v_m = 3.2 x 10^{-3} m s^{-1}; t_e = 10 min; t_m = 2 min; n = 3

Tables

Table 1: Performed hMSC-TERT cultivations in fixed-bed bioreactors at different scales. Bold-faced cultivations were used for the model verification in part B of this study.

Fixed-bed volume V_{FB} [cm^3]	Growth surface A_{FB} [cm^2]	Inoculated cell density [cm^{-2}]	Medium volume V_{CV} [ml]	Superficial velocity v [m s^{-1}]	Medium changes [h]	Cultivation time [h]
4 x 14.2	**4 x 260**	**10,000**	**1,000**	**2.65 x 10^{-4}**	**115**	**135**
4 x 14.2	4 x 260	10,000	1,000	7.96 x 10^{-4}	93	134
4 x 14.2	4 x 260	10,000	1,000	15.92 x 10^{-4}	105	138
60	**1098**	**7,000**	**500**	**3.0 x 10^{-4}**	**-**	**168**
300	**5490**	**10,000**	**4,800**	**(0.8 - 3.3) x 10^{-4}**	**149**	**167**

Table 2: Overview of the harvesting experiments performed in fixed-bed reactors at a scale of 14.2 cm^3. A: Accutase™ solution, T: trypsin solution (0.25% in PBS without calcium and magnesium)

Enzyme	Superficial velocity, enzyme solution v_e [m s^{-1}]	Duration of perfusion with the enzyme solution t_e [min]	Superficial velocity, medium v_m [m s^{-1}]	Duration of perfusion with medium t_m [min]	Method
A	8.00 x 10^{-4}	10	-	-	cyclic perfusion of enzyme solution
A	1.58 x 10^{-3}	10	-	-	
A	3.18 x 10^{-3}	20	-	-	
A	1.83 x 10^{-4}	10	1.58 x 10^{-3}	1	non-cyclic perfusion of enzyme solution and medium (directly led to the collecting vessel)
A	1.83 x 10^{-4}	10	1.58 x 10^{-3}	2	
A	1.83 x 10^{-4}	10	3.17 x 10^{-3}	1	
A	1.83 x 10^{-4}	10	3.17 x 10^{-3}	2	
A+T*	1.83 x 10^{-4}	10	1.58 x 10^{-3}	2	
A+T*	1.83 x 10^{-4}	10	3.17 x 10^{-3}	2	

*1:1 v/v

Table 3: Published growth kinetics of several cell types.

Cell type	Growth rate [d^{-1}]	Monod constant [mg ml^{-1}]	Reference
Adipose stem cells (rhesus monkey)	0.37 (passage 11) 0.23 (passage 14)	-	[24]
Mesenchymal stem cells (human)	0.66 - 0.94	-	[28]
Mesenchymal stem cells (human)	0.5	-	[29]
Mesenchymal stem cells (human)	0.55	-	[30]
Myeloma cell line X63-Ag8.653 (murine)	1.56	0.13	[31]
Mesodermal progenitor cells (human)	0.33 - 1.3	-	[32]
Embryoicl stem cell line H9 (human)	0.47	-	[33]

Table 4: Published glucose consumption kinetics of several cell types.

Cell type	Glucose consumption rate [mg $^{-1}$ h^{-1} $cell^{-1}$]	Monod constant [mg ml^{-1}]	Reference
Embryonic stem cell line S25 (murine)	(0.9 - 1.88) x 10^{-8}	-	[7]
Mesenchymal stem cells (human)	(2.25 - 6.9) x 10^{-8}	-	[28]
CHO (hamster)	8.46 x 10^{-8}	-	[34]
Hybridoma cell line 4C10B6 (murine)	(0.13 - 1.37) x 10^{-7}	-	[35]
Mesenchymal stem cells (human)	1.22 x 10^{-7}	-	[36]
Leucemic cell line K562 (human)	1.59 x 10^{-7}	-	[37]
Vero (Chlorocebus)	2.4 x 10^{-8}	0.1	[38]

Table 5: Results of the hMSC-TERT cultivation in 2-mm borosilicate glass spheres comprising fixed-bed reactors.

	Units	V_{FB} = 4 x 14.2 cm^3	V_{FB} = 60 cm^3	V_{FB} = 300 cm^3
Cultivation time	[h]	135	168	167,3
End cell density X_{FB}^{n}	[cm^{-2}]	(1.60 ± 0.06) x 10^5	9.56 x 10^4	1.12 x 10^5
	[cm^{-3}]	(2.93 ± 0.11) x 10^6	1.75 x 10^6	2.05 x 10^6
Passage number	-	68	71	84
Superficial velocity v	[m s^{-1}]	2.7 x 10^{-4}	3.0 x 10^{-4}	(0.8 - 3.3) x 10^{-4}
Lactate/glucose	[mg/mg]	1.61	0.80	0.93
	[mol/mol]	3.22	1.60	1.86
Initial cell density * X_A^0 and X_{FB}^0	[cm^{-2}]	(5.64 ± 0.50) x 10^3	(3.68 ± 0.99) x 10^3	(6.39 ± 0.66) x 10^3
	[cm^{-3}]	(1.03 ± 0.09) x 10^4	(6.63 ± 1.81) x 10^4	(1.17 ± 0.12) x 10^5
Mean growth rate * μ_{m}	[d^{-1}]	0.60 ± 0.02	0.49 ± 0.04	0.42 ± 0.02
Mean glucose consumption rate * $q_{Glc,\mathrm{m}}$	[mg h^{-1} cell^{-1}]	(7.65 ± 0.3) x 10^{-8}	(6.80 ± 0.43) x 10^{-8}	(9.50 ± 0.27) x 10^{-8}
* Correlation coefficient	[-]	0.999	0.998	0.924

Oxygen consumption rate q_{Ox}	[mg h^{-1} $cell^{-1}$]	2.03 x 10^{-8}	2.06 x 10^{-8}	1.08 x 10^{-8}

Table 6: Published oxygen consumption kinetics of several cell types.

Cell type	Oxygen consumption rate [mg h^{-1} $cell^{-1}$]	Monod constant [mg ml]	Reference
Adherent mononuclear cells from bone marrow (human)	(1.22 ± 0,19) x 10^{-8}	-	[39]
Skin fibroblasts (rat)	1.88 x 10^{-8}	2.0 x 10^{-4}	[40]
Hematopoietic stem cells (human)	1.92 x 10^{-8}	-	[41]
Breast cancer stem cells (human)	(3.2 ± 0,07) x 10^{-8}	(2.3 ± 0.5) x 10^{-3}	[42]
Hybridoma cell line 4H11 (murine-human)	1.1 x 10^{-8}	-	[43]

Figures

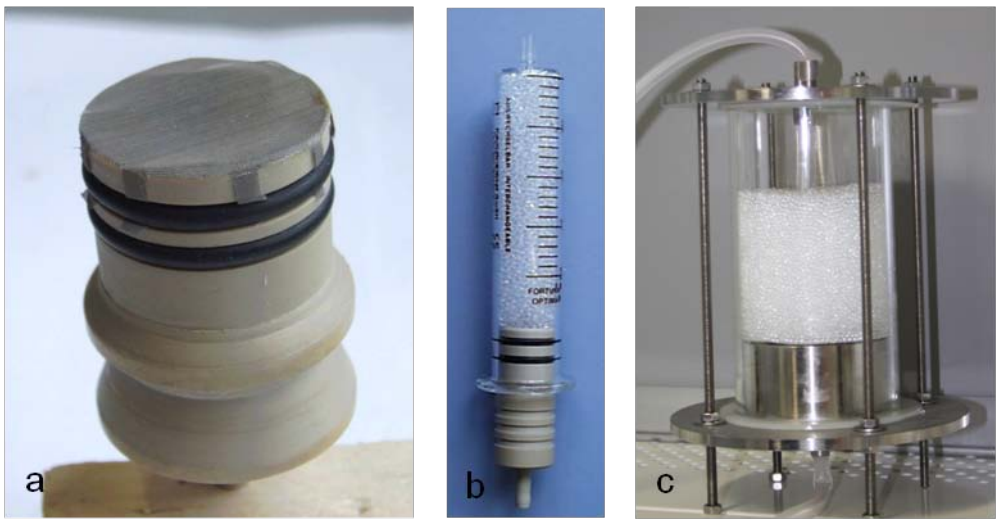

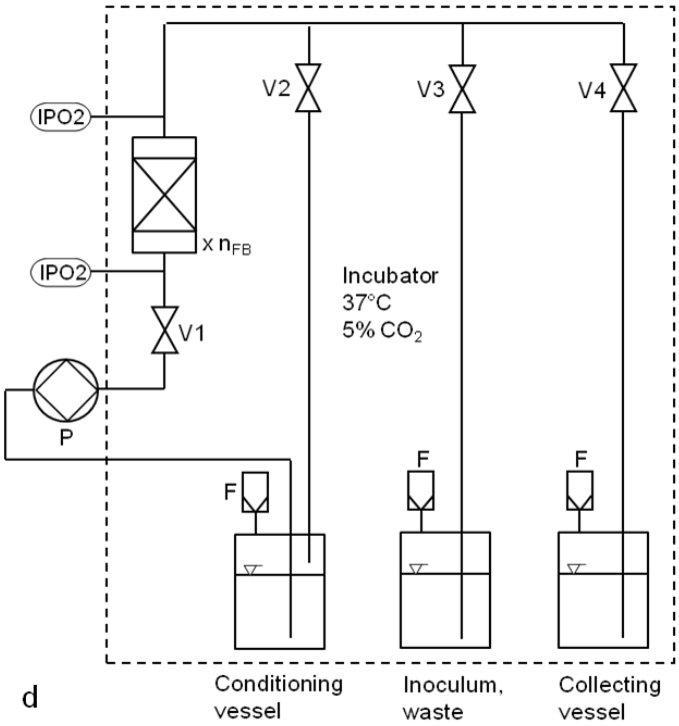

Figure 1

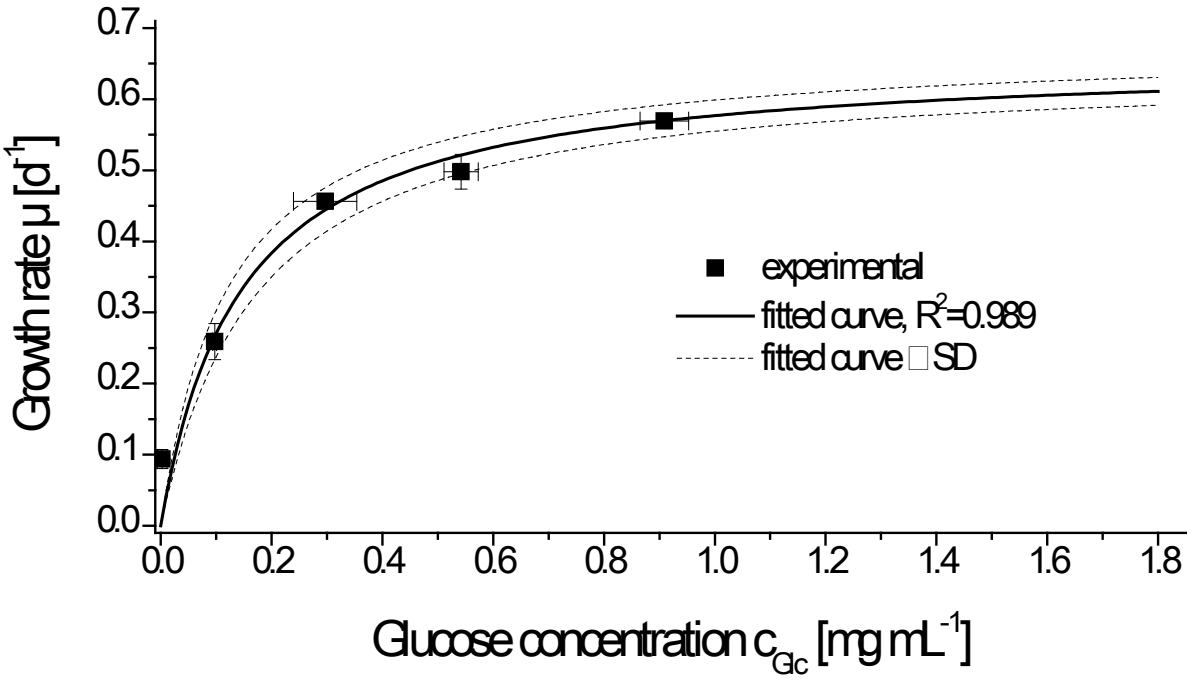
Growth rate μ [d-1]
0.0
0.1
0.2
0.3
0.4
0.5
0.6
0.7
0.0
0.2
0.4
0.6
0.8
1.0
1.2
1.4
1.6
1.8
Glucose concentration cGlc [mg mL-1]
experimental
fitted curve, R2=0.989
fitted curve ± SD

Figure 2

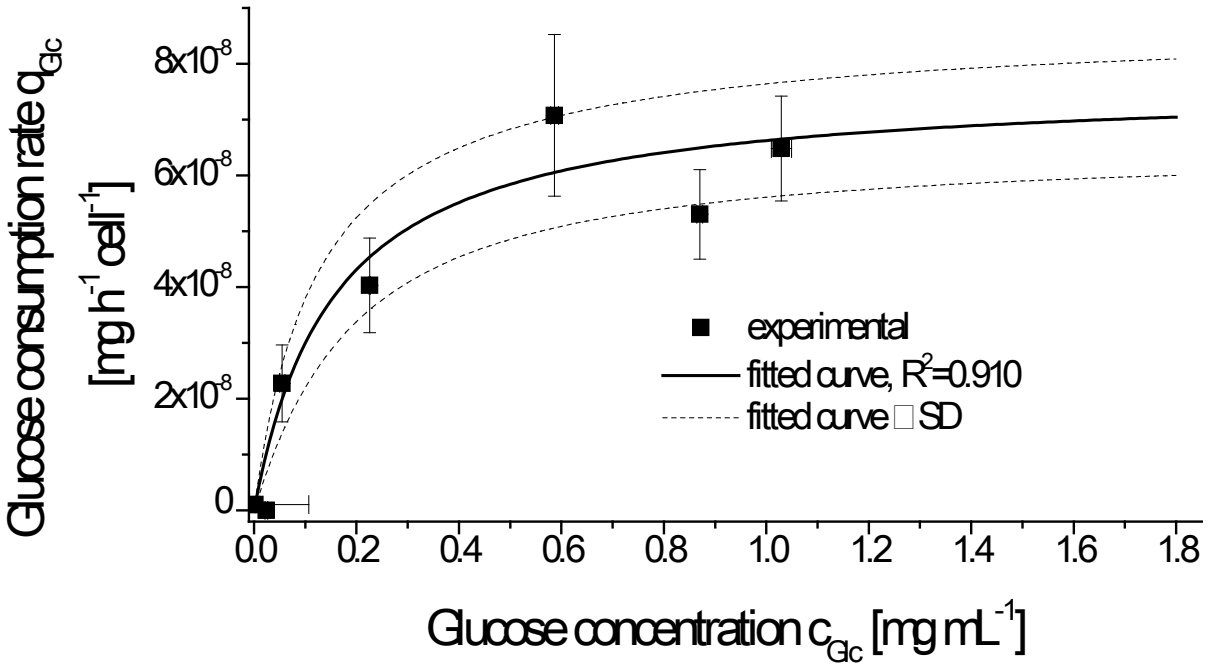
Glucose consumption rate q_{Glc} [mg h^{-1} cell^{-1}]
8x10^{-8}
6x10^{-8}
4x10^{-8}
2x10^{-8}
0
0.0
0.2
0.4
0.6
0.8
1.0
1.2
1.4
1.6
1.8
Glucose concentration c_{Glc} [mg mL^{-1}]
experimental
fitted curve, R^2=0.910
fitted curve ± SD

Figure 3

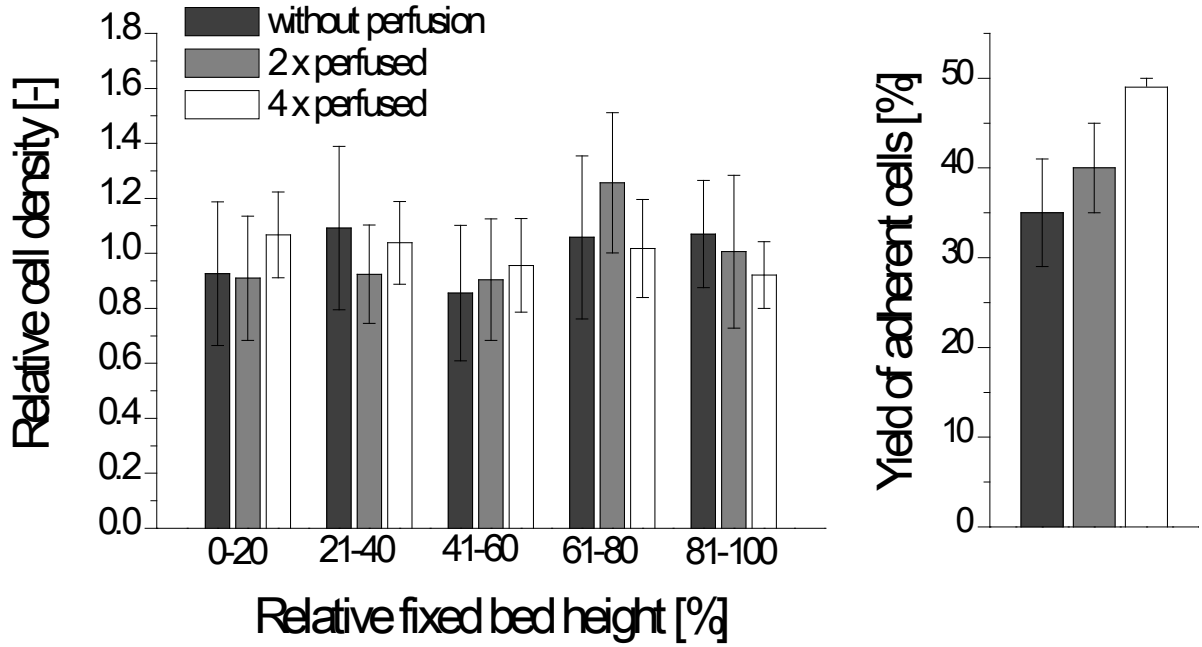
without perfusion
2 x perfused
4 x perfused
Relative cell density [-]
1.8
1.6
1.4
1.2
1.0
0.8
0.6
0.4
0.2
0.0
0-20
21-40
41-60
61-80
81-100
Relative fixed bed height [%]
Yield of adherent cells [%]
50
40
30
20
10
0

Figure 4

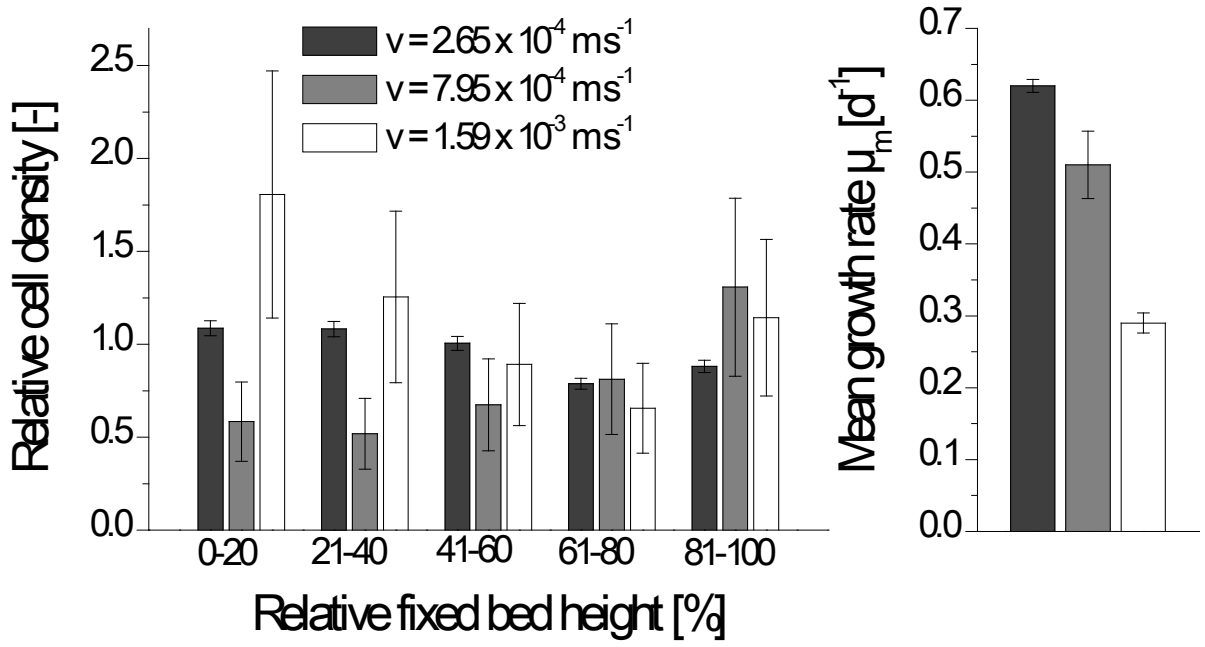
v = 2.65 x 10-4 ms-1
v = 7.95 x 10-4 ms-1
v = 1.59 x 10-3 ms-1
Relative cell density [-]
0.0
0.5
1.0
1.5
2.0
2.5
0-20
21-40
41-60
61-80
81-100
Relative fixed bed height [%]
Mean growth rate μm [d-1]
0.0
0.1
0.2
0.3
0.4
0.5
0.6
0.7

Figure 5

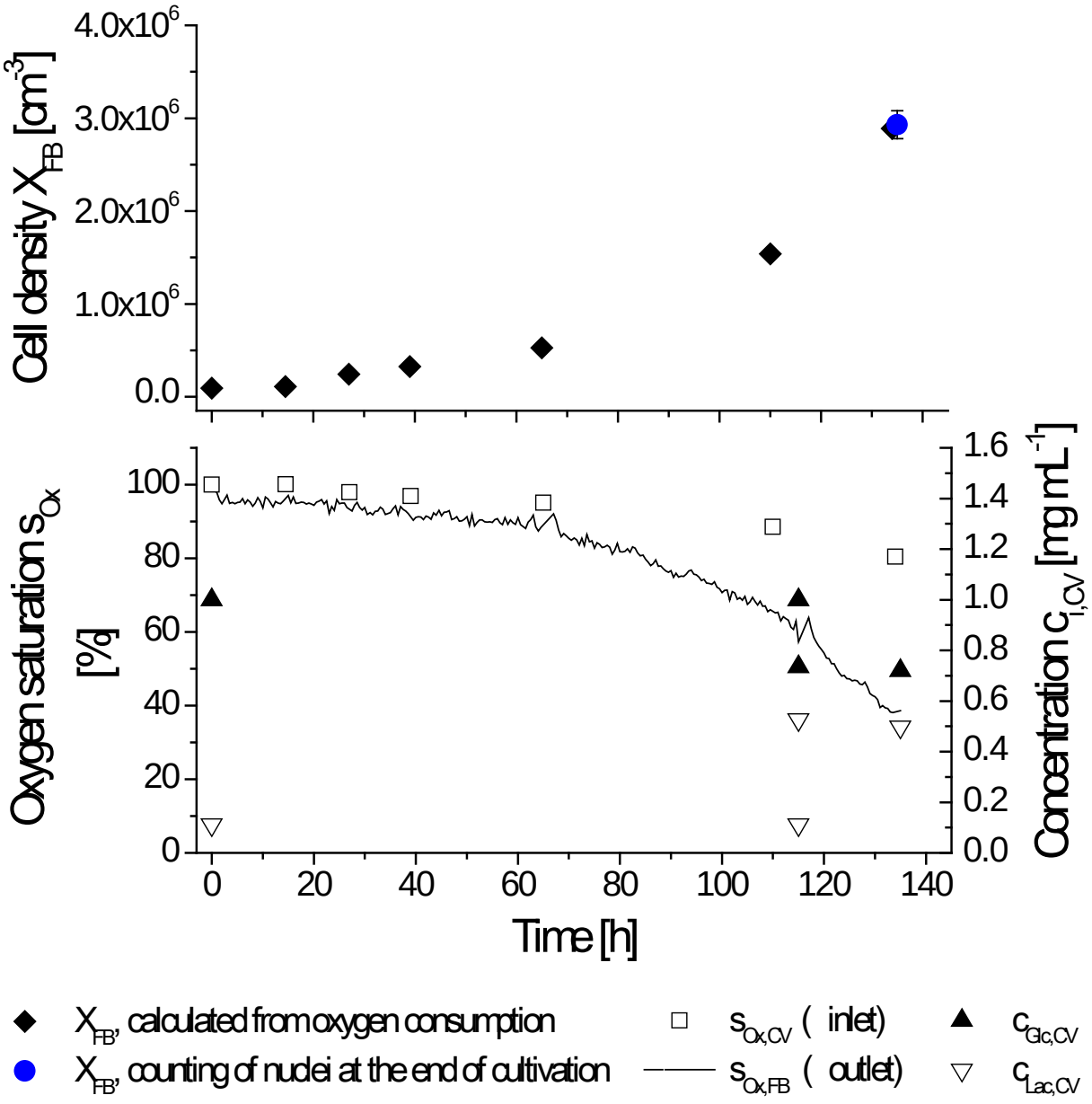
Cell density X_{FB} [cm^{-3}]
4.0x10^6
3.0x10^6
2.0x10^6
1.0x10^6
0.0
Oxygen saturation s_{Ox} [%]
100
80
60
40
20
0
Concentration $c_{i,CV}$ [mg mL^{-1}]
1.6
1.4
1.2
1.0
0.8
0.6
0.4
0.2
0.0
0
20
40
60
80
100
120
140
Time [h]
X_{FB}, calculated from oxygen consumption
X_{FB}, counting of nuclei at the end of cultivation
$s_{Ox,CV}$ (inlet)
$s_{Ox,FB}$ (outlet)
$c_{Glc,CV}$
$c_{Lac,CV}$

Figure 6

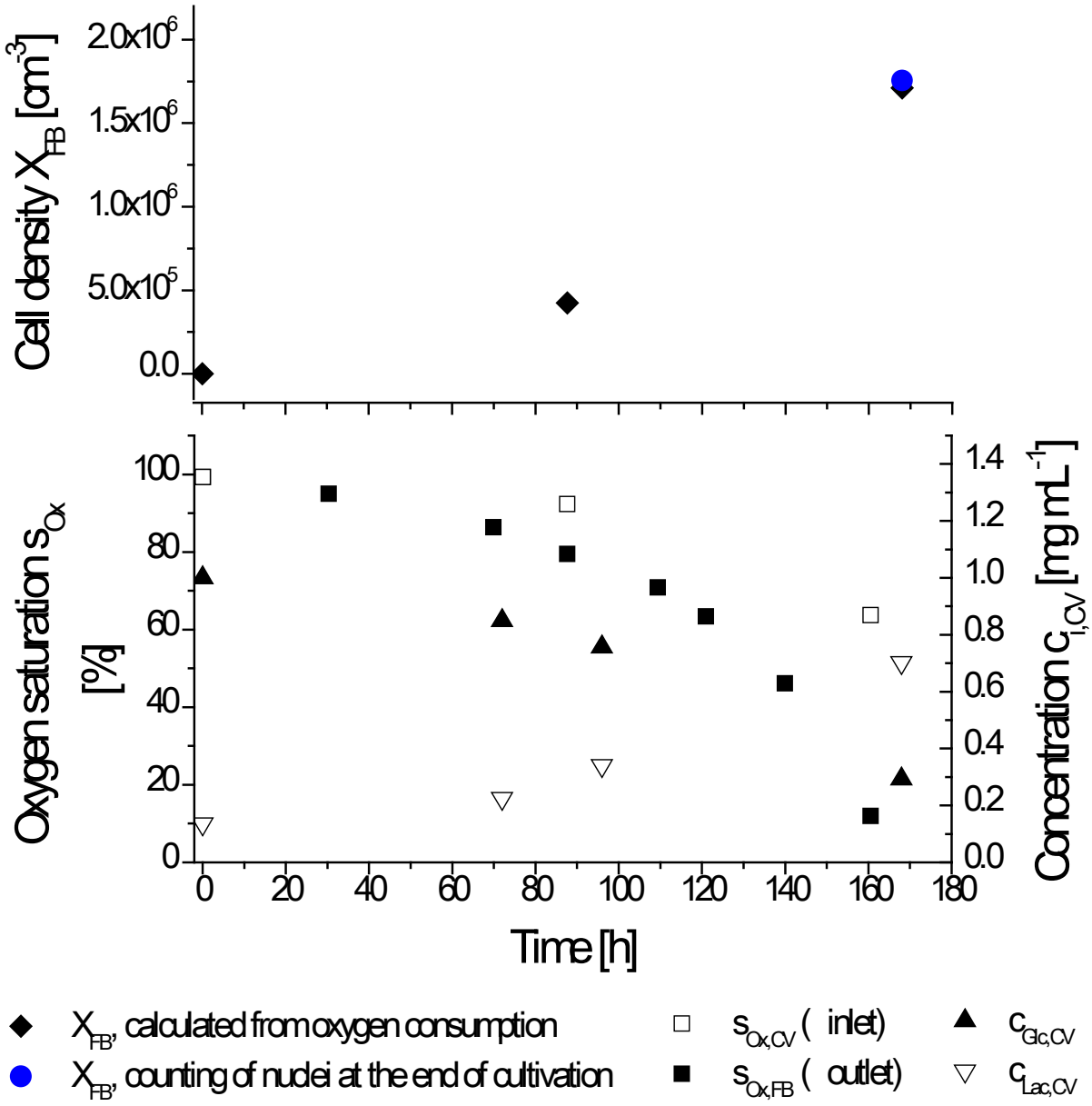
Cell density X_{FB} [cm^{-3}]
2.0x10^6
1.5x10^6
1.0x10^6
5.0x10^5
0.0
Oxygen saturation s_{Ox} [%]
100
80
60
40
20
0
Concentration $c_{i,CV}$ [mg mL^{-1}]
1.4
1.2
1.0
0.8
0.6
0.4
0.2
0.0
0
20
40
60
80
100
120
140
160
180
Time [h]
X_{FB}, calculated from oxygen consumption
X_{FB}, counting of nuclei at the end of cultivation
$s_{Ox,CV}$ (inlet)
$s_{Ox,FB}$ (outlet)
$c_{Glc,CV}$
$c_{Lac,CV}$

Figure 7

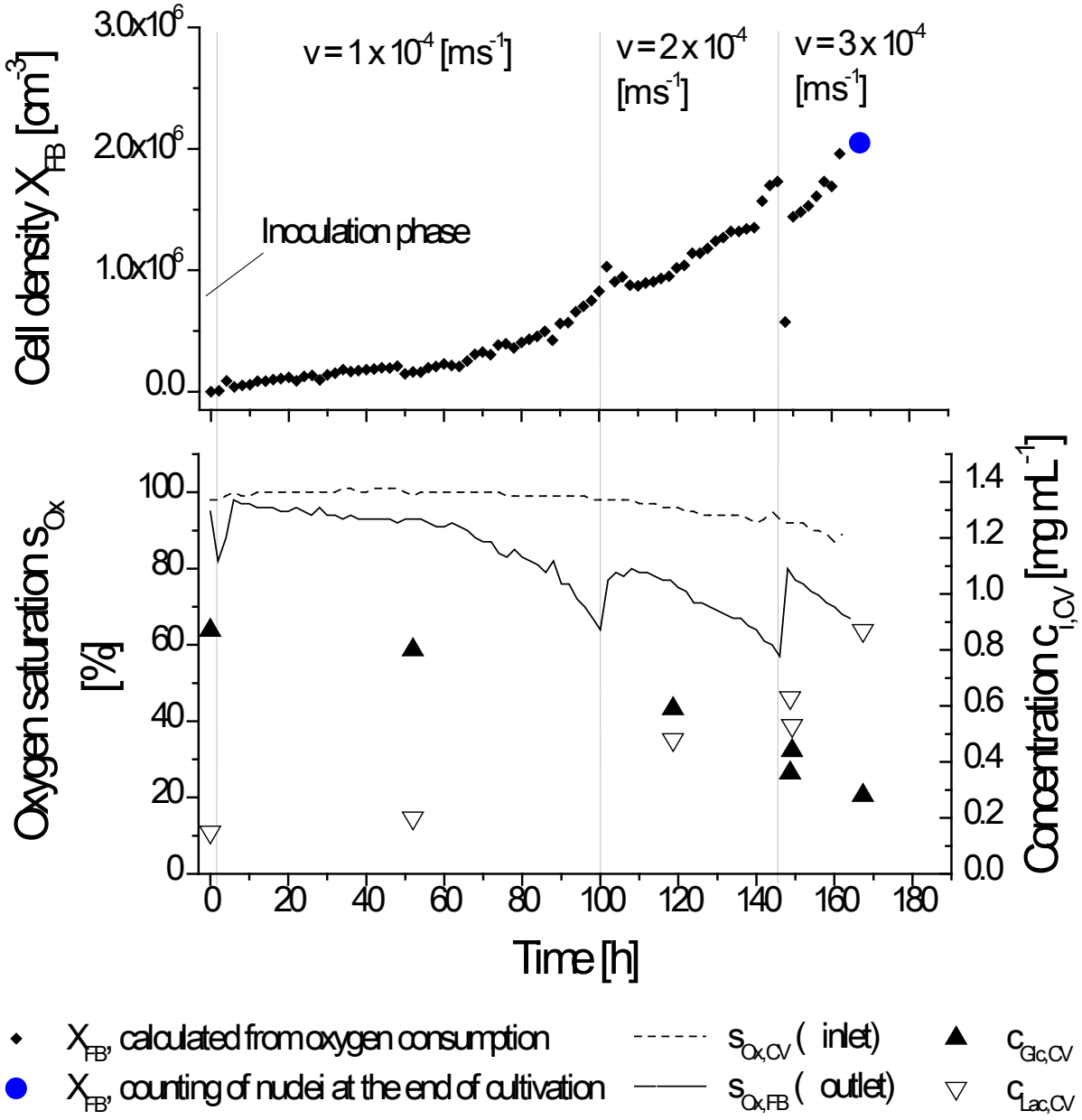
Cell density X_{FB} [cm^{-3}]
3.0x10^6
2.0x10^6
1.0x10^6
0.0
v = 1 x 10^{-4} [ms^{-1}]
v = 2 x 10^{-4} [ms^{-1}]
v = 3 x 10^{-4} [ms^{-1}]
Inoculation phase
Oxygen saturation s_{Ox} [%]
100
80
60
40
20
0
Concentration $c_{i,CV}$ [mg mL^{-1}]
1.4
1.2
1.0
0.8
0.6
0.4
0.2
0.0
0
20
40
60
80
100
120
140
160
180
Time [h]
X_{FB}, calculated from oxygen consumption
X_{FB}, counting of nuclei at the end of cultivation
$s_{Ox,CV}$ (inlet)
$s_{Ox,FB}$ (outlet)
$c_{Glc,CV}$
$c_{Lac,CV}$

Figure 8

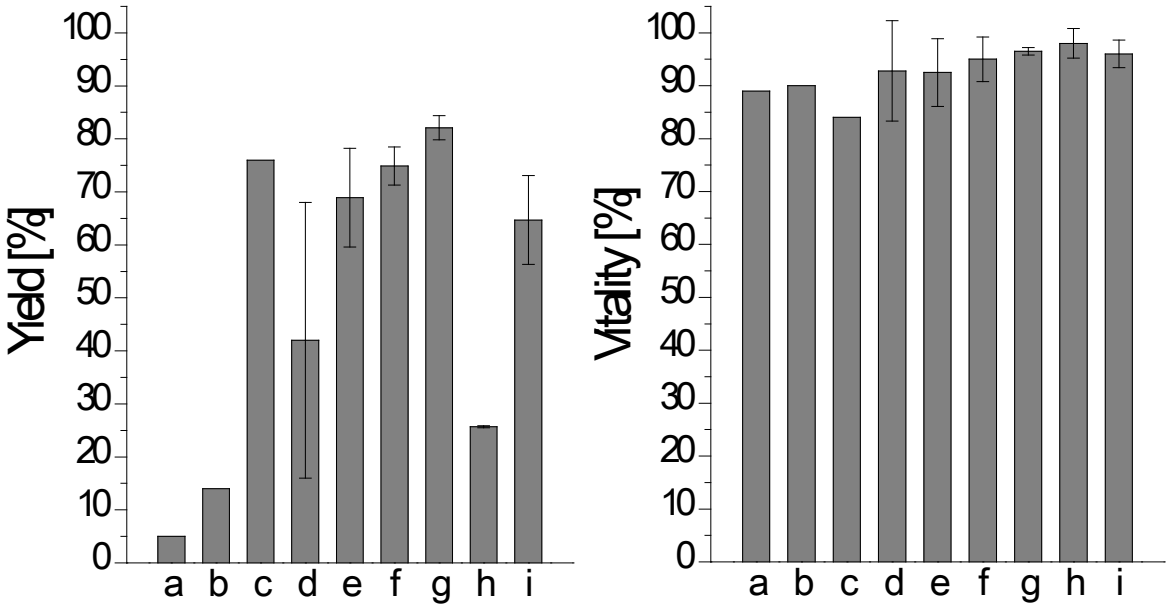
Yield [%]
100
90
80
70
60
50
40
30
20
10
0
a b c d e f g h i
Vitality [%]
100
90
80
70
60
50
40
30
20
10
0
a b c d e f g h i

Figure 9